Original Article: Laboratory Investigation

Early dynamics of circulating tumor DNA predict clinical response to immune checkpoint inhibitors in metastatic renal cell carcinoma

Yoko Koh,[1] (iD) Kosuke Nakano,[1] Kotoe Katayama,[2] Gaku Yamamichi,[1] Satoru Yumiba,[1]
Eisuke Tomiyama,[1] (iD) Makoto Matsushita,[1] Yujiro Hayashi,[1] Yoshiyuki Yamamoto,[1] Taigo Kato,[1] (iD)
Koji Hatano,[1] Atsunari Kawashima,[1] (iD) Takeshi Ujike,[1] Ryoichi Imamura,[1] Rui Yamaguchi,[2,3,4]
Seiya Imoto,[2] Yukimasa Shiotsu,[5] Norio Nonomura[1] and Motohide Uemura[1]

[1]Department of Urology, Osaka University Graduate School of Medicine, Suita, Osaka, [2]Division of Health Medical Intelligence, Human Genome Center, The Institute of Medical Science, The University of Tokyo, Minato-ku, Tokyo, [3]Division of Cancer Systems Biology, Aichi Cancer Center Research Institute, [4]Division of Cancer Informatics, Nagoya University Graduate School of Medicine, Nagoya, Aichi, Japan, and [5]Guardant Health Inc., Redwood City, California, USA

Abbreviations & Acronyms
ccRCC = clear cell renal cell carcinoma
cfDNA = cell-free DNA
CHIP = clonal hematopoiesis of indeterminate potential
CNA = copy number amplification
CR = complete response
ctDNA = circulating tumor DNA
DNA = deoxyribonucleic acid
DEL = deletion
ICI = immune checkpoint inhibitor
Indels = insertions/deletions
INS = insertion
irAE = immune-related adverse event
MAF = mutant allele frequency
mRCC = metastatic renal cell carcinoma
NA = not available
NGS = next-generation sequencing
NR = nonresponder
PD = progressive disease
PD-L1 = programmed death-ligand 1
PFS = progression free survival
PR = partial response
SD = stable disease
SNV = single nucleotide variant
TB = tumor burden
TMB = tumor mutation burden
WES = whole exome sequencing

Correspondence: Motohide Uemura M.D., Ph.D., M.B.A., Department of Urology, Osaka University Graduate School of Medicine, 2-2 Yamadaoka, Suita, Osaka 565-0871, Japan. Email: uemura@uro.med.osaka-u.ac.jp

Address of the institution at which the work was carried out: Department of Urology, Osaka University Graduate School of Medicine, 2-2 Yamadaoka, Suita, Osaka 565-0871, Japan.

Objectives: Detection of genomic alterations in circulating tumor deoxyribonucleic acid of peripheral blood can guide the selection of systemic therapy in cancer patients. The predictive significance of circulating tumor deoxyribonucleic acid in metastatic renal cell carcinoma remains unclear, especially for patients treated with immune checkpoint inhibitors.

Methods: In this study, we collected plasma samples before and 1 month after commencing nivolumab monotherapy or nivolumab plus ipilimumab therapy from 14 metastatic renal cell carcinoma patients. We performed circulating tumor deoxyribonucleic acid genomic profiling in plasma cell-free deoxyribonucleic acid by next-generation sequencing using a commercially available pan-cancer panel (Guardant360 CDx). Additionally, we also performed whole exome sequencing of tumor tissues and compared the concordance of genomic profiles with circulating tumor deoxyribonucleic acid.

Results: Nine patients had circulating tumor deoxyribonucleic acid in pretreatment plasma samples with a total of 20 mutations (15 single nucleotide variants, three insertions/deletions, and two copy number amplification). *VHL* (30.0%) was the most frequently mutated gene, followed by *TP53* (20.0%), and 45.0% of circulating tumor deoxyribonucleic acid mutations were concordant with somatic mutations in tumor tissues. Patients with decreasing circulating tumor deoxyribonucleic acid mutant allele frequency had better progression free survival when compared to those with increasing mutant allele frequency ($P = 0.0441$).

Conclusions: Our findings revealed that early circulating tumor deoxyribonucleic acid dynamics can serve as a predictive biomarker for response to immune checkpoint inhibitors in metastatic renal cell carcinoma patients.

Key words: biomarker, circulating tumor DNA, clear cell renal cell carcinoma, immune checkpoint inhibitor, next-generation sequencing.

Introduction

ICIs have revolutionized the management of cancer and improved the patient's prognosis over the past decade.[1] However, the response rates of ICIs are still limited[2] and the majority of patients have no benefit from ICI treatments, occasionally with severe irAEs.[3] So far, numerous biomarkers including PD-L1 expression, TMB, and lymphocyte infiltration in cancer tissues have been proposed to have a significant impact on the therapeutic response to ICIs.[4] However, no biomarker for mRCC has yet been developed in ICI therapy due to a number of complicating issues including tumor heterogeneity and the various types of settings in clinical studies.[4,5] In addition, conventional radiographic imaging may be unfit to evaluate the efficacy of ICI therapy due to unique tumor responses such as pseudo-progression or durable response.[6] Thus, there is an urgent need for biomarkers to predict the efficacy of ICIs to avoid unnecessary treatment.

Liquid biopsy is becoming an essential resource to provide information on the biological characteristics of cancer with minimum invasiveness, which enables longitudinal and real-time monitoring when compared to cancer tissue-based tests in oncology.[7–10] In particular, with the advancement of NGS technology, ctDNA receives plenty of attention, which detects cancer-related genomic alterations in peripheral blood. Using NGS-based ctDNA analysis, several studies recently demonstrated that early ctDNA dynamics could serve as a predictive biomarker for responses to ICI therapy in other tumor types.[11–14] However, the utility of ctDNA as a predictive biomarker for RCC has not yet been demonstrated although ICIs are key drugs for treating mRCC in clinical settings.

Recently, a deep sequencing platform of cfDNA has improved the detection rates of ctDNA in mRCC.[15] Given this advancement of technology, we analyzed ctDNA in 14 mRCC patients with programmed cell death-1 inhibitor-based therapy by means of the newest commercially available gene panel assay. We also performed tissue-based WES analysis and compared the concordance of genomic profiles with ctDNA. Our findings revealed that the gene panel in this study had adequate detectability for ctDNA and early ctDNA dynamics could practically predict the clinical efficacy in mRCC.

Methods

Study design

In this study, we enrolled 14 patients with ccRCC who initiated ICI therapy between April 2017 and May 2020. This study was approved by the Institutional Review Board of Osaka University Hospital (#12187-5, #13397-19 and #668-4). All patients provided written informed consent.

Blood samples were collected before treatment (pre) and at 1 month after the initiation of the treatment (M1). All patients were pathologically diagnosed with ccRCC by surgical resection or needle biopsy of the primary tumor. Histopathological diagnosis was performed based on standard hematoxylin and eosin-stained sections, as assessed by two or more experienced senior pathologists, according to the 8th Union for International Cancer Control TNM staging system.[16]

Assessment of clinical response to ICI therapy

Objective response was evaluated by computed tomography or magnetic resonance-based imaging using RECIST v1.1.[17] Taking distinctive radiographical responses of ICI therapy into consideration, we defined responders and NR as follows. Responders were patients who achieved CR, PR, or SD (≥6 months). We also defined responders as patients with durable response more than 6 months after discontinuation of ICI therapy due to adverse events or unrelated disease. NR were defined as patients with SD (<6 months) or PD. As a result, responders and NRs consisted of seven and seven cases, respectively.

Detection of ctDNA

Whole blood samples were collected in EDTA tubes. Blood samples were centrifuged at 900 and 20 000 rpm for 10 min sequentially and supernatants were stored at −80°C as plasma. A total of 1–2 mL of plasma was used for cfDNA sequencing.

All cfDNA extraction, processing, and sequencing was performed in a CLIA-certified, CAP-accredited laboratory (Guardant Health, Inc., Redwood City, CA, USA). We extracted cfDNA using the QIAGEN QIAsymphony SP Instrument and reagent system. The resulting cfDNA is quantified using the 4200 TapeStation (Agilent, Santa Clara, CA, USA). Up to 30 ng of extracted cfDNA from the plasma was labeled with nonrandom oligonucleotide barcodes and was used to prepare sequencing libraries, which were then enriched by hybrid capture, pooled, and sequenced using NGS as previously described.[18] Sequencing data were analyzed using the proprietary Guardant360 bioinformatics pipeline designed to detect SNVs, indels, CNAs and fusions.

Whole exome sequencing

RCC tissues obtained from surgical resection were frozen and preserved at −80°C. Tumor tissues from needle biopsy were also soaked in RNAlater (Thermo Fisher Scientific, Waltham, MA, USA) and stored at −20°C until use. Tumor DNA was isolated from these frozen tissues using Allprep DNA/RNA mini kit (QIAGEN, Hilden, Germany). Germline DNA was isolated from 200 μL aliquots of whole blood samples using QIAamp DNA Blood Mini Kit (QIAGEN).

WES of tumor and germline DNA was performed using target capture with Agilent SureSelect XT Human All Exon V6 (Agilent Technologies, Santa Clara, CA, USA). The raw sequence data were generated by the Illumina NovaSeq6000 platform (Illumina, San Diego, CA, USA) with a standard 150-bp paired-end read protocol at Macrogen Japan (Tokyo, Japan).

FASTQ files were generated by bcl2fastq2 (v.2.20.0) for our sequence data. Somatic mutations in tumor DNA and germline mutations were identified using the Genomon pipeline (https://github.com/Genomon-Project/genomon-docs/tree/v2.6.3). GRCh37 was used as the reference genome. Of the mutations detected in tumor DNA, mutations overlapping with germline mutations were excluded as SNPs or errors. We used the following criteria: (i) Fisher's exact $P \leq 0.1$, (ii) ≥4 variant reads in the tumor sample, (iii) MAF in the tumor sample ≥0.02, and (iv) MAF of the matched normal sample <0.1, with the exclusion of synonymous SNVs and known variants listed in NCBI dbSNP build 131. For the tissue-based WES analysis, TMB was defined as the total number of somatic mutations including SNVs and indels.

Assessment of early ctDNA dynamics

Early ctDNA dynamics were analyzed in patients positive for ctDNA at either or both pre and M1. Early ctDNA dynamics were defined as changes in the maximum MAF of SNV or indel mutations between pre- and M1-plasma samples. Mutant allele fraction, which is defined as the ratio of mutated to nonmutated DNA that is sequenced for any specific genomic position included in Guradant360, are reported quantitatively for somatic SNVs of clinical significance and

distinguished from germline SNVs by reference to the COS-MIC and dbSNP databases, as well as their concentrations.

Statistical analysis

Statistical analysis was performed in R (v.4.0.3). The comparison between responders and NRs was performed with Mann–Whitney *U* test for continuous data (pakage 'exactRankTests' v.0.8-31) and Fisher's exact test for categorical data. Kaplan–Meier method was used to estimate the survival rate using the 'survival' package (v.3.2-7). PFS was calculated as the duration from the initiation of the treatment to disease progression. Responders and NRs were compared using log-rank test. The R package 'ggplot2' (v.3.3.3) was used to draw the line charts, the bar charts, and dot plots. The landscape of somatic mutations was generated using the R package 'GenVisR' (v.1.22.1). *P* value of <0.05 was considered statistically significant.

Results

Patient characteristics

The clinical and pathological characteristics were summarized in Table 1. The median age was 66.5 years (range 45–80 years). The majority (85.7%) of patients had one or two metastatic sites, and the most common metastatic site was lung (71.4%). Ten patients received nivolumab monotherapy and had previously received an antiangiogenic agent. Four patients received nivolumab plus ipilimumab therapy as first-line therapy. ICI therapy proceeded for a median of 262 days (range 40–827 days), and the median follow-up duration was 554 days (range 171–1392 days). The objective response rate was 14.3% (2 out of 14 patients). The median PFS and OS were 172.5 days (range 25–1301 days) and 262 days (range 40–827 days), respectively. A total of nine patients experienced irAEs and three patients permanently discontinued ICI therapy due to irAEs.

Clinical significance of plasma cfDNA in mRCC patients

We analyzed cfDNA in 28 samples (both pre- and M1-plasma samples, results were summarized in Table S1) by Guardant360. We successfully extracted at least 5 ng cfDNA from all but two samples (median amount 12.1 ng, range 4.4–31.2 ng) despite low plasma volume (range 1.0–1.9 mL). Sequencing was successfully performed for all but one sample, from which only 4.3 ng cfDNA was extracted. The overview of the sequencing analysis is indicated in Figure 1. We successfully analyzed both pre- and M1-plasma cfDNA samples in 13 patients.

Next, we measured the dynamics of cfDNA before and during treatment to determine whether the dynamics could predict the clinical response to ICIs (Fig. 2a). The median cfDNA concentration was 7.8 ng/mL in preplasma samples (range 2.4–16.7 ng/mL) and 9.6 ng/mL in M1-plasma samples (range 3.2–20.8 ng/mL). As a result, we found that the ratio of M1/precfDNA concentration was significantly decreased in responders versus NRs (*P* = 0.0175; Fig. 2b).

Table 1 Patient characteristics of entire cohort (*n* = 14) and ctDNA analysis cohort (*n* = 11)

	Total (*n* = 14)	ctDNA analysis (*n* = 11)
Age, years, median (range)	66.5 (45–80)	68 (45–80)
Sex		
Male	11	8
Female	3	3
Clinical stage at initial diagnosis		
I	2	2
III	3	3
IV	9	6
Tissue collection		
Nephrectomy	13	10
Biopsy	1	1
Progression pattern		
Synchronous metastases	7	6
Metachronous metastases	6	5
International metastatic RCC database consortium criteria		
Intermediate	10	9
Poor	4	2
Sites of metastasis		
Lung	10	8
Bone	4	3
Liver	3	3
Adrenal gland	3	2
Others	6	4
Previous medical history		
None	4	2
Antiangiogenic agent	10	9
ICI therapy		
Nivolumab	10	9
Nivolumab + ipilimumab	4	2
irAE		
None	5	5
Grade 1	2	2
Grade 2	1	0
Grade 3	6	4
Treatment duration, days, median (range)	262 (40–827)	357 (40–827)
Follow-up term, days, median (range)	554 (171–1392)	556 (171–1301)

Identification of plasma ctDNA in mRCC patients

Among 13 patients with successful cfDNA sequencing, 11 patients had detectable ctDNA. CtDNA was identified in pre-plasma samples in nine of these patients (Fig. 1). To eliminate false-positives caused by detection of CHIP, we compared ctDNA profiles with germline and somatic mutations detected by WES. We identified one missense mutation in *IDH2* R140Q (MAF 12.28%) as a CHIP variant in patient K108. This *IDH2* mutation was not detected in somatic mutations derived from tumor tissue. Besides this *IDH2* mutation, a total of 20 mutations were detected in preplasma samples (Fig. 3). The commonly mutated genes in two or more patients were *VHL* (30.0%), *TP53* (20.0%), *ATM* (10.0%), and *MET* (10.0%). No microsatellite instability-high was detected in pre- nor M1-plasma samples.

```
mRCC: 14 patients (pre 14 samples, M1 14 samples)
```

```
Sequencing failure: 1 patient
pre failure and M1 success
```

```
Sequencing success in both pre and M1 samples: 13 patients
```

```
ctDNA negative: 2 patients
```

```
Analysis for ctDNA dynamics: 11 patients
    ctDNA positive in both pre and M1 samples: 8 patients
    ctDNA positive only in pre sample: 1 patient
    ctDNA positive only in M1 sample: 2 patients
```
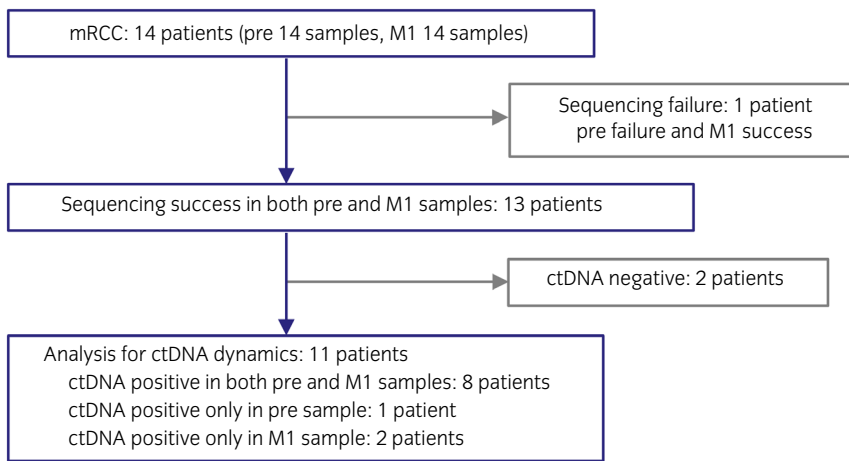
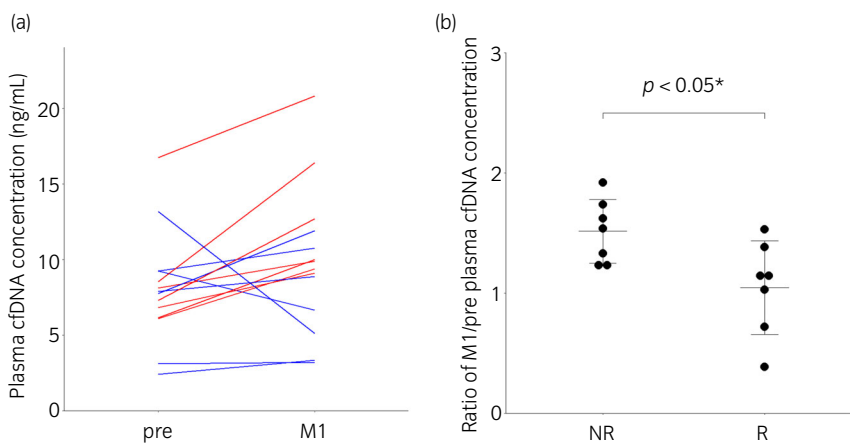Fig. 1 The overview of cfDNA sequencing analysis.

Fig. 2 The clinical significance of plasma cfDNA concentration in mRCC patients treated with ICIs. (a) Concentration changes in plasma cfDNA between pre- and M1-plasma samples in 14 patients are represented. Red lines indicate changes in NR ($n = 7$), and blue lines for responders (R; $n = 7$). (b) The ratio of M1 to pre plasma cfDNA concentration between NR and R ($n = 14$). *$P < 0.05$ (Mann–Whitney U test). Central line, mean; error bars, standard deviation.

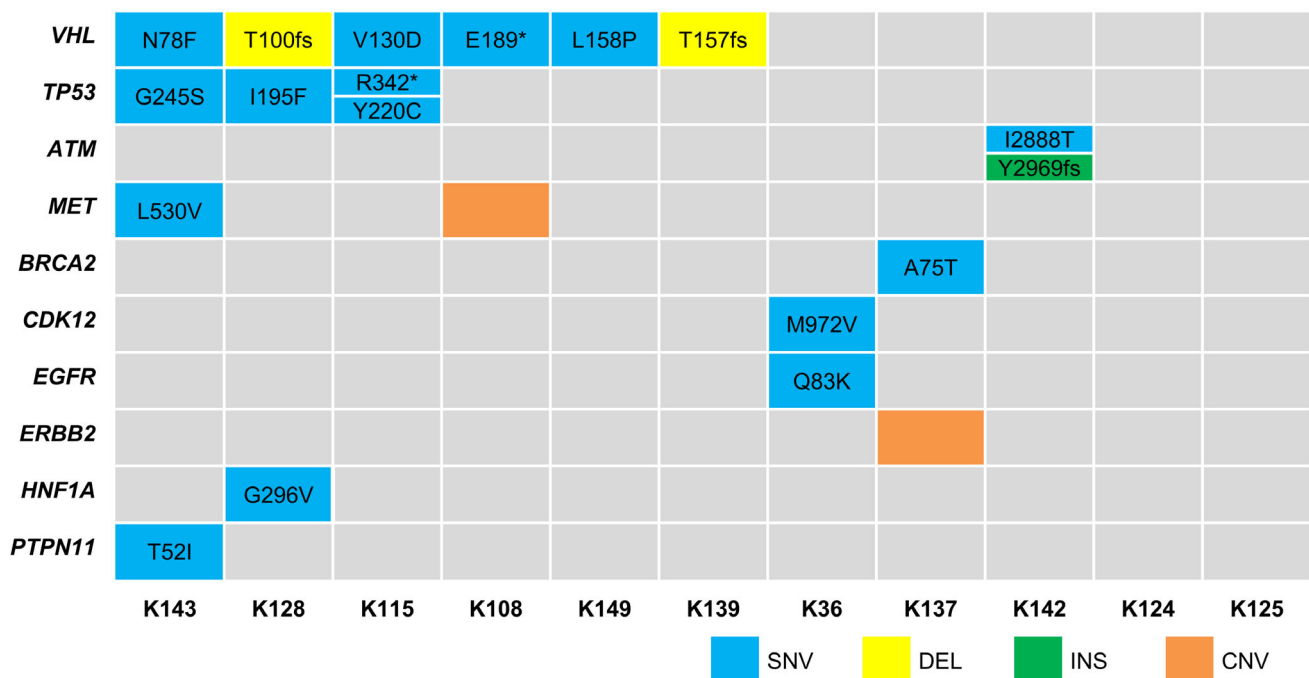|	K143	K128	K115	K108	K149	K139	K36	K137	K142	K124	K125
VHL	N78F	T100fs	V130D	E189*	L158P	T157fs					
TP53	G245S	I195F	R342* / Y220C								
ATM									I2888T / Y2969fs		
MET	L530V			(CNV)							
BRCA2								A75T			
CDK12							M972V				
EGFR							Q83K				
ERBB2								(CNV)			
HNF1A		G296V									
PTPN11	T52I										

SNV | DEL | INS | CNV

Fig. 3 The landscape of mutated genes identified in pre-samples for each ctDNA positive patient is shown. K124 and K125 were positive for ctDNA only in M1 samples. Sequence changes are indicated in the cells.

Concordance between plasma cfDNA sequencing and tissue-based WES

We performed tissue-based WES in all 14 patients. Figure S1a lists the mutations detected in at least two patients. The most frequently mutated gene was *VHL* (64.3%), followed by *PBRM1* (50.0%) and *BAP1* (35.7%). We also found that the median TMB was 48 (range 17–185), with no significant difference in value between responders and NRs (*P* = 0.134; Fig. S1b).

Next, we explored the concordance of mutational profiles between plasma ctDNA and tumor DNA. Of 20 mutations identified in plasma ctDNA, nine mutations (45.0%) were consistent with somatic mutations detected in WES of tumor DNA (Fig. 4a). When focusing on 73 genes of interest in the panel of cfDNA sequencing, we found *VHL* in nine, *TP53* in two, and *MET* in two of 14 patients among somatic mutations detected via tissue-based WES (Fig. 4b), which resulted in the coincidence rate with ctDNA of 55.6%, 100%, and 50%, respectively.

Early ctDNA dynamics predicted clinical response to ICI therapy

Next, we investigated whether early ctDNA dynamics predicted clinical response to ICI therapy. Early ctDNA dynamics of all patients are depicted in Figure S2, and clinical course is summarized in Figure 5. Based on the criteria of this study, the cohort was divided into six NRs and five responders. The decrease of ctDNA was confirmed in four patients among five responders, while the increase of ctDNA was confirmed in five patients among six NRs (Figs 5,6a), it has indicated that MAF tended to decrease more frequently in responders compared with NRs (*P* = 0.0801, Fisher's exact test; Fig. 6a). Importantly, PFS after the first administration of ICIs was significantly longer in patients with decreasing ctDNA levels than those with increasing ctDNA levels (*P* = 0.0441; Fig. 6b).

The clinical course of ctDNA dynamics and radiographic findings in two patients, one responder and one NR, are described in Figure 7. Patient K36 (Fig. 7a) showed a decreasing trend of TB within SD range at the first radiographic assessment. Although the treatment was discontinued due to irAE, K36 maintained PR for 30 months. In this case, the decreasing trend in MAF of ctDNA predicted the clinical outcome prior to conventional radiographic imaging. In contrast, K125 had an increase in ctDNA MAF with PD detected by CT imaging 13 weeks later. In this patient, the treatment was switched to axitinib with clinical benefit according to the initial assessment.

Discussion

Recently, the development of cancer treatments has imposed molecular profiling for patients in order to achieve precision cancer medicine. Liquid biopsy is an emerging approach to
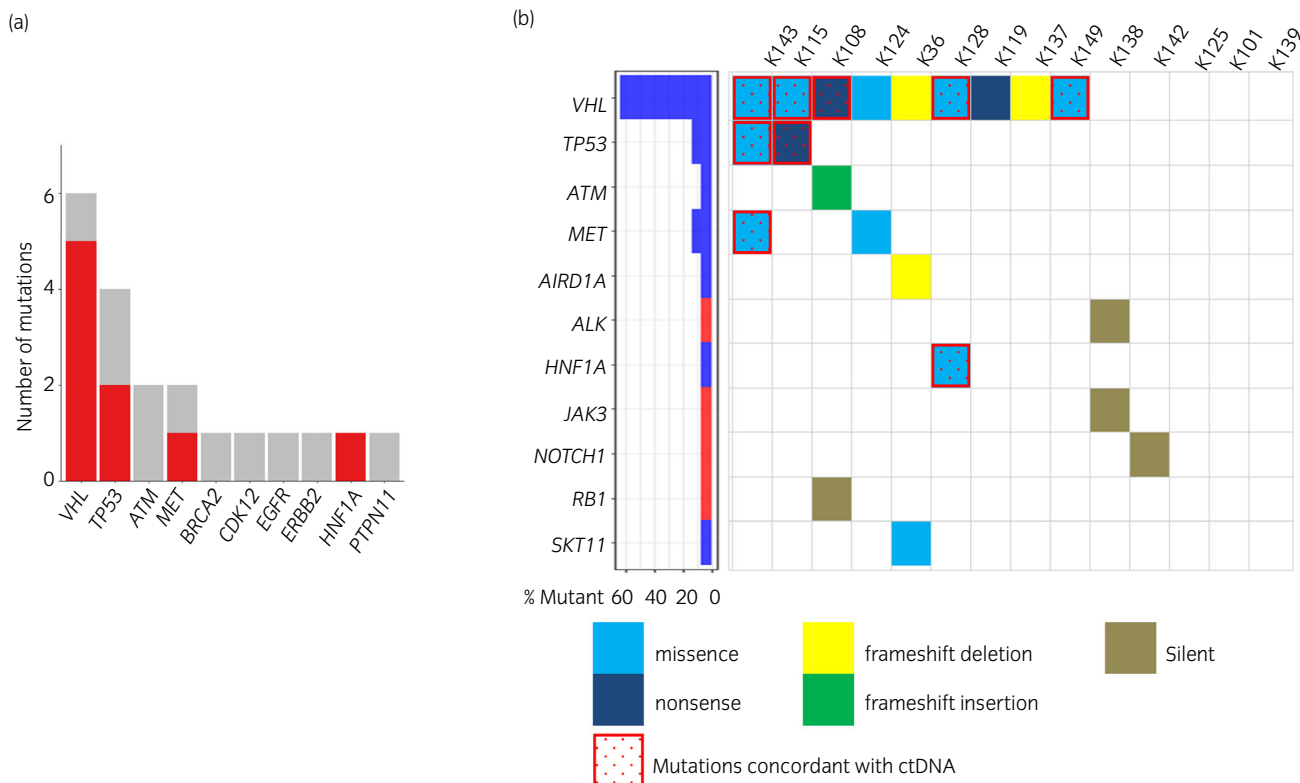

Fig. 4 (a) Bar chart shows the number of mutations of each gene concordant with mutations detected by WES of tumor DNA (red) among 20 mutations detected in ctDNA. The color gray shows mutations that are not consistent with WES. (b) The mutation plot of tissue-based WES analysis focusing on the 73 genes of interest in the pan-cancer panel for cfDNA sequencing. The color blue and red in the left panel represents nonsynonymous and synonymous mutation respectively.
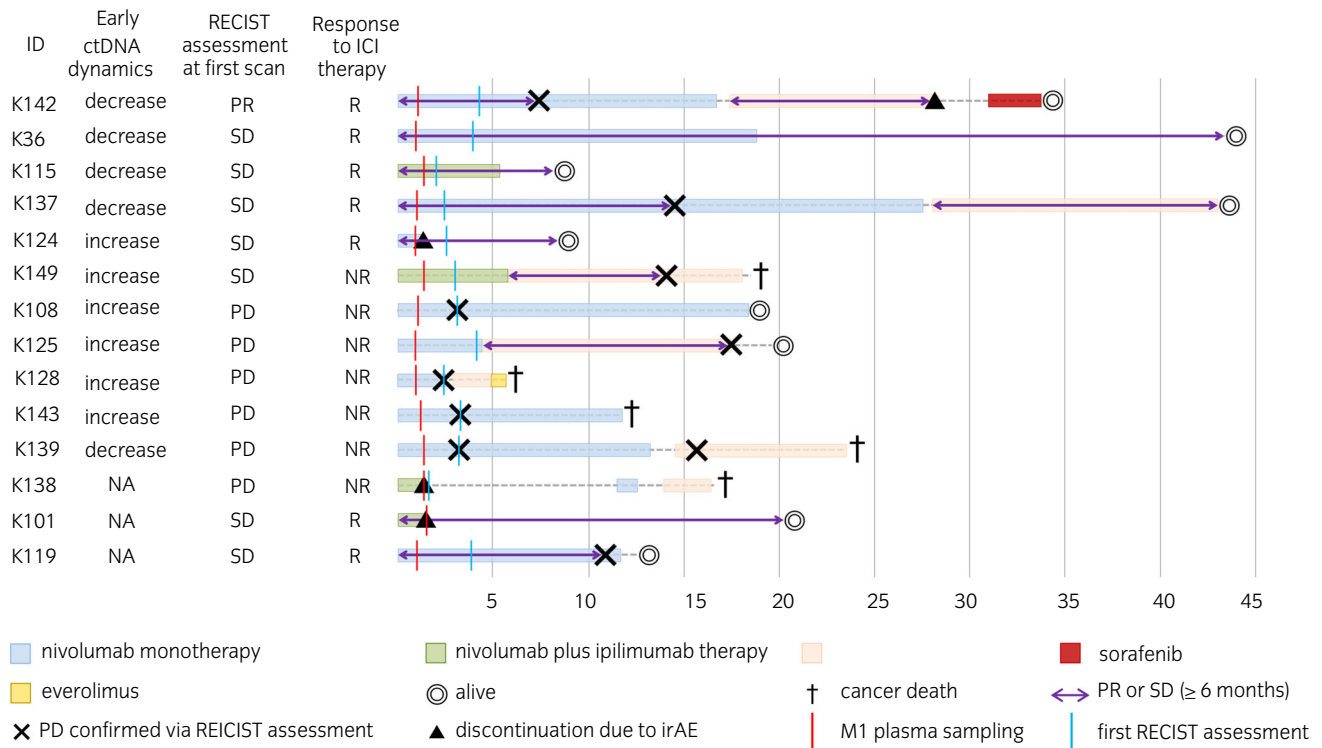
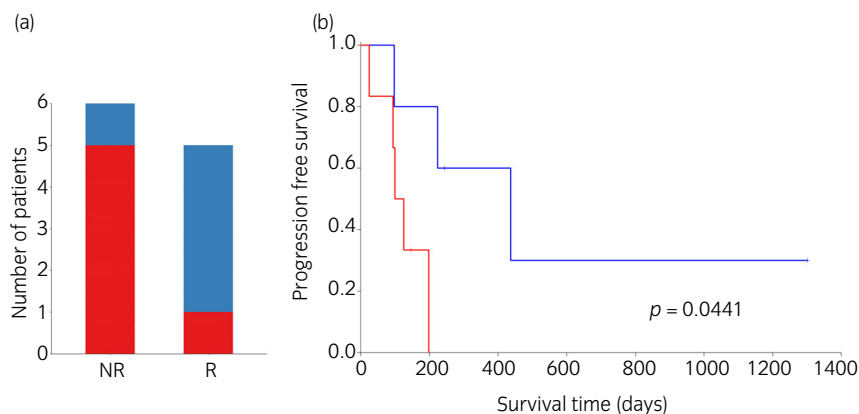Fig. 5 Clinical course of all 14 patients. R, responder.

Fig. 6 The clinical significance of early ctDNA dynamics in ICI therapy. The maximum MAF of ctDNA mutations changed before and after the initiation of ICI. (a) Bar chart represents the classification of increase/decrease in maximum MAF of ctDNA between responders (R) and NR. $P = 0.0801$ (Fisher's exact test). (b) Association of early ctDNA dynamics (increase vs decrease) for PFS. The blue line represents patients with decreasing in MAF, and red with increasing in MAF.

providing cancer genomic information with minimum invasiveness.[19] In particular, analysis of ctDNA has undergone remarkable development as a useful biomarker for cancer genotyping, in some cases replacing tissue-based approaches.[8] However, there have been only a few reports for plasma ctDNA in RCC since ctDNA levels are considered to be limited even in the advanced stage of disease. The technological innovation of cfDNA sequencing has improved the detection rates of ctDNA in mRCC.[20] Hence, in this study, we investigated the performance value of tissue agnostic cfDNA sequencing assay for mRCC. Furthermore, we aimed to confirm the diagnostic potential of ctDNA as a biomarker for predicting the efficacy of ICI therapy for mRCC.

We have demonstrated several novel findings that show the usefulness of ctDNA in mRCC through ctDNA analysis

of this study. First, we found that ctDNA was detected in either pre- or M1-samples in 11 out of 14 patients (78.6%). In general, the detection rate of ctDNA has been reported to be <70.0% in RCC.[21–23] The digital sequencing platform of the pan-cancer panel used in this study enabled ultra-high specificity leading to complete sequencing of all or the critical exons in covered genes.[24] This technique remarkably improved the detection rate of ctDNA in mRCC.[15] In addition, the concordance rate of mutations identified in plasma ctDNA to those detected in tissue-based WES was 45.0% (Fig. 4b). Due to tumor heterogeneity within and between metastatic sites, tissue-based WES may not be able to detect all mutations in the entire tumor and only reflects the information at the time of specimen collection.[9] On the other hand, cfDNA sequencing could reflect real-time tumor status
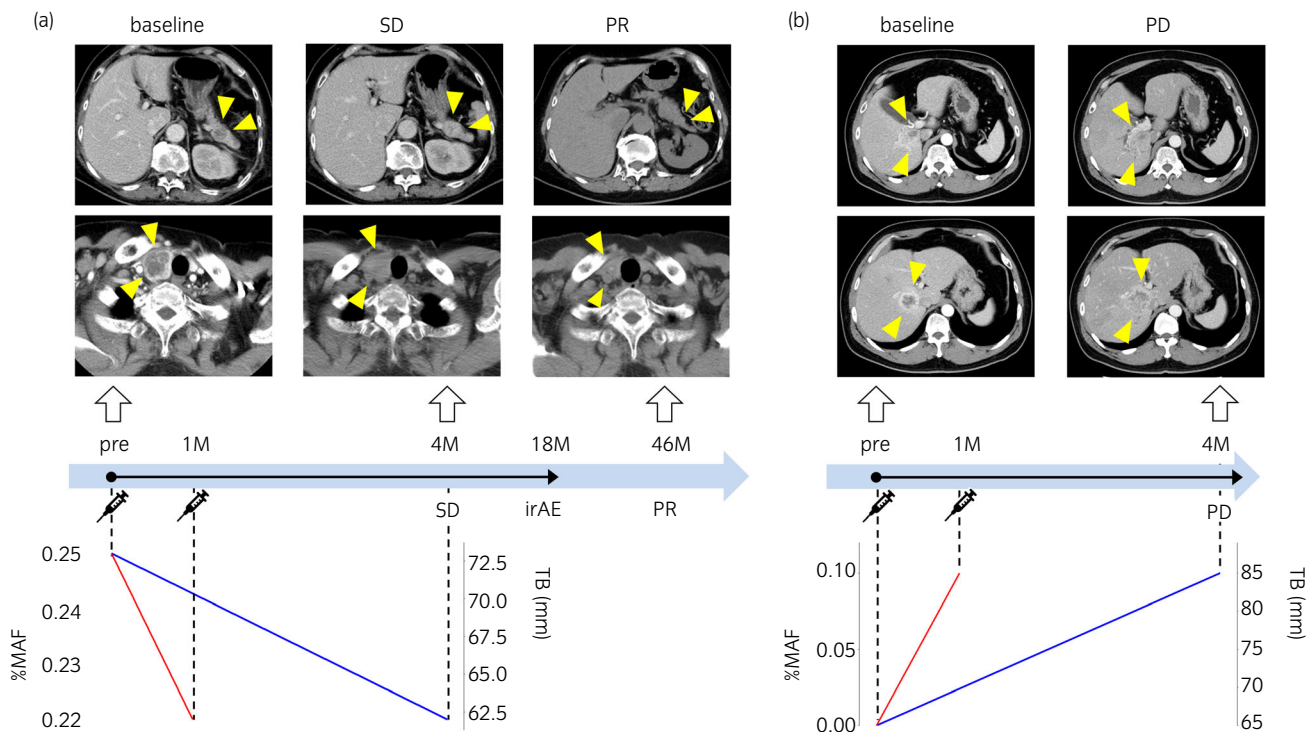
Fig. 7 Monitoring maximum MAF of ctDNA and radiographic findings along clinical course in mRCC patients treated with ICIs. The black arrow overlaid on the blue arrow indicates the duration of ICI therapy. Line charts represent changes in maximum MAF of ctDNA between pre- and M1-plasma samples (red) and changes in radiographic TB according to the RECIST v.1.1 criteria (blue). (a) K36 was a long-term responder with no progression after discontinuing the treatment due to an irAE. (b) K125 was a typical NR demonstrating an increase in both MAF of ctDNA and RECIST TB at the first assessment.

and overcome the problems of tissue-based WES. Thus, the performance of cfDNA sequencing was considered to be useful for mRCC.

Second, we have clarified that early ctDNA dynamics could predict clinical response to ICI therapy and was significantly associated with PFS (Fig. 6a,b). Several groups reported that ctDNA dynamics in the early phase of the treatment could predict clinical response to ICIs in multiple cancer types.[11–14] For example, Nabet *et al.*[12] demonstrated that ctDNA dynamics after one cycle of ICI could predict early response in nonsmall cell lung carcinoma. In our study, we found that the early ctDNA dynamics were associated with response to ICI therapy in nine of 11 patients, but it was not significantly different probably due to small number of patients. In those cases, ctDNA changes reflected treatment effects much earlier than the confirmation of assessment via conventional radiographic imaging. Although we were only able to measure plasma ctDNA at two points in this study, serial analysis of plasma ctDNA along the clinical course may lead to the establishment of biomarkers for monitoring disease activity more sensitively and dynamically than radiographic imaging. In the future, liquid biopsy will be applied to various clinical markers, such as early detection of cancer and treatment selection, as well as prediction of efficacy as a minimally invasive, repeatable, and comprehensive tool to understand the nature of the entire tumor.

There were several limitations in the present study. The patient characteristics were heterogeneous with its retrospective nature. The cohort included both patients treated with nivolumab monotherapy and nivolumab plus ipilimumab therapy. Therefore, we were unable to rule out the effect of ipilimumab completely. In addition, the number of patients was small and the statistical validity is weak. Further investigations are necessary to validate our results in a larger cohort of patients by multi-institutional studies.

Nevertheless, our findings in mRCC are consistent with studies in other tumor types that measured ctDNA dynamics in patients treated with ICIs.[11–14] Our results imply that the pan-cancer panel used here has sufficient detectability for ctDNA, and that early ctDNA dynamics during ICI therapy may be a promising biomarker to predict response to ICI treatment in mRCC patients.

Acknowledgments

Author contributions

Yoko Koh: Conceptualization; Data curation; Formal analysis; Funding acquisition; Investigation; Methodology; Validation; Visualization; Writing – original draft; Writing – review & editing. Kosuke Nakano: Conceptualization; Resources. Kotoe Katayama: Data curation; Formal analysis; Software; Writing – review & editing. Gaku Yamamichi: Data curation;

Formal analysis. Satoru Yumiba: Data curation; Formal analysis. Eisuke Tomiyama: Data curation; Formal analysis; Writing – review & editing. Makoto Matsushita: Data curation; Formal analysis. Yujiro Hayashi: Data curation; Formal analysis. Yoshiyuki Yamamoto: Data curation; Formal analysis. Taigo Kato: Formal analysis; Writing – review & editing. Koji Hatano: Formal analysis; Writing – review & editing. Atsunari Kawashima: Formal analysis. Takeshi Ujike: Formal analysis. Ryoichi Imamura: Supervision. Rui Yamaguchi: Formal analysis; Software. Seiya Imoto: Formal analysis; Software. Yukimasa Shiotsu: Conceptualization; Data curation; Formal analysis; Project administration; Supervision; Writing – review & editing. Norio Nonomura: Supervision. Motohide Uemura: Conceptualization; Formal analysis; Funding acquisition; Project administration; Writing – review & editing.

Conflict of interest

None declared.

Approval of the research protocol by an Institutional Reviewer Board

The protocol for this research has been approved by the Institutional Review Board of Osaka University Hospital (Approval No. #12187-5, #13397-19 and #668-4).

Informed consent

All patients provided written informed consent.

Registry and the Registration No. of the study/trial

N/A.

Animal studies

N/A.

References

1 Braun DA, Bakouny Z, Hirsch L *et al*. Beyond conventional immune-checkpoint inhibition – novel immunotherapies for renal cell carcinoma. *Nat. Rev. Clin. Oncol.* 2021; **18**: 199–214.

2 Yip SM, Wells C, Moreira R *et al*. Checkpoint inhibitors in patients with metastatic renal cell carcinoma: results from the International Metastatic Renal Cell Carcinoma Database Consortium. *Cancer* 2018; **124**: 3677–83.

3 Postow MA, Sidlow R, Hellmann MD. Immune-related adverse events associated with immune checkpoint blockade. *N. Engl. J. Med.* 2018; **378**: 158–68.

4 Guida A, Sabbatini R, Gibellini L, De Biasi S, Cossarizza A, Porta C. Finding predictive factors for immunotherapy in metastatic renal-cell carcinoma: what are we looking for? *Cancer Treat. Rev.* 2021; **94**: 102157.

5 Choueiri TK, Motzer RJ. Systemic therapy for metastatic renal-cell carcinoma. *N. Engl. J. Med.* 2017; **376**: 354–66.

6 Seymour L, Bogaerts J, Perrone A *et al*. iRECIST: guidelines for response criteria for use in trials testing immunotherapeutics. *Lancet Oncol.* 2017; **18**: e143–52.

7 Merker JD, Oxnard GR, Compton C *et al*. Circulating tumor DNA analysis in patients with cancer: American Society of Clinical Oncology and College of American Pathologists Joint Review. *J. Clin. Oncol.* 2018; **36**: 1631–41.

8 Heitzer E, Haque IS, Roberts CES, Speicher MR. Current and future perspectives of liquid biopsies in genomics-driven oncology. *Nat. Rev. Genet.* 2019; **20**: 71–88.

9 Kilgour E, Rothwell DG, Brady G, Dive C. Liquid biopsy-based biomarkers of treatment response and resistance. *Cancer Cell* 2020; **37**: 485–95.

10 Nakano K, Yamamoto Y, Yamamichi G *et al*. Fragmentation of cell-free DNA is induced by upper-tract urothelial carcinoma-associated systemic inflammation. *Cancer Sci.* 2021; **112**: 168–77.

11 Goldberg SB, Narayan A, Kole AJ *et al*. Early assessment of lung cancer immunotherapy response via circulating tumor DNA. *Clin. Cancer Res.* 2018; **24**: 1872–80.

12 Nabet BY, Esfahani MS, Moding EJ *et al*. Noninvasive early identification of therapeutic benefit from immune checkpoint inhibition. *Cell* 2020; **183**: 363–76.e313.

13 Jin Y, Chen D-L, Wang F *et al*. The predicting role of circulating tumor DNA landscape in gastric cancer patients treated with immune checkpoint inhibitors. *Mol. Cancer* 2020; **154**: https://doi.org/10.1186/s12943-020-01274-7.

14 Zhang QU, Luo J, Wu S *et al*. Prognostic and predictive impact of circulating tumor DNA in patients with advanced cancers treated with immune checkpoint blockade. *Cancer Discov.* 2020; **10**: 1842–53.

15 Zill OA, Banks KC, Fairclough SR *et al*. The landscape of actionable genomic alterations in cell-free circulating tumor DNA from 21,807 advanced cancer patients. *Clin. Cancer Res.* 2018; **24**: 3528–38.

16 Brierley JD. *TNM Classification of Malignant Tumours*, 8th edn. Union for International Cancer Control, Geneva, Switzerland, 2017.

17 Eisenhauer EA, Therasse P, Bogaerts J *et al*. New response evaluation criteria in solid tumours: revised RECIST guideline (version 1.1). *Eur. J. Cancer* 2009; **45**: 228–47.

18 Odegaard JI, Vincent JJ, Mortimer S *et al*. Validation of a plasma-based comprehensive cancer genotyping assay utilizing orthogonal tissue- and plasma-based methodologies. *Clin. Cancer Res.* 2018; **24**: 3539–49.

19 Siravegna G, Mussolin B, Venesio T *et al*. How liquid biopsies can change clinical practice in oncology. *Ann. Oncol.* 2019; **30**: 1580–90.

20 Pal SK, Sonpavde G, Agarwal N *et al*. Evolution of circulating tumor DNA profile from first-line to subsequent therapy in metastatic renal cell carcinoma. *Eur. Urol.* 2017; **72**: 557–64.

21 Zhang Y, Yao YU, Xu Y *et al*. Pan-cancer circulating tumor DNA detection in over 10,000 Chinese patients. *Nat. Commun.* 2021; **12**: 11.

22 Bettegowda C, Sausen M, Leary RJ *et al*. Detection of circulating tumor DNA in early- and late-stage human malignancies. *Sci. Transl. Med.* 2014; **6**: 224.

23 Yamamoto Y, Uemura M, Fujita M *et al*. Clinical significance of the mutational landscape and fragmentation of circulating tumor DNA in renal cell carcinoma. *Cancer Sci.* 2019; **110**: 617–28.

24 Lanman RB, Mortimer SA, Zill OA *et al*. Analytical and clinical validation of a digital sequencing panel for quantitative, highly accurate evaluation of cell-free circulating tumor DNA. *PLoS One* 2015; **10**: e0140712.

Supporting information

Additional Supporting Information may be found in the online version of this article at the publisher's web-site:

Figure S1. (a) The landscape of somatic mutations detected by WES of tumor DNA. The status of somatic mutations common to at least two or more patients is shown. K139 had no mutation which was shared in other patients. (b) Association between TMB and clinical response to ICI therapy ($n = 14$; $P = 0.134$, Mann–Whitney U test).

Figure S2. Line charts represent changes of maximum MAF in all ctDNA mutations between pre- and M1-samples in each patient who had positive ctDNA ($n = 11$).

Table S1. Raw data of cfDNA sequencing analysis.